6. J. S. Takahashi, *Annu. Rev. Neurosci.* **18**, 531 (1995).
7. M. A. Rea, *Brain Res. Bull.* **23**, 577 (1989); B. Rusak, H. A. Robertson, W. Wisden, S. P. Hunt, *Science* **248**, 1237 (1990); J. M. Kornhauser, D. E. Nelson, K. E. Mayo, J. S. Takashashi, *Neuron* **5**, 127 (1990); B. Rusak, L. McNaughton, H. A. Robertson, S. P. Hunt, *Mol. Brain Res.* **14**, 124 (1992); J. M. Kornhauser, D. E. Nelson, K. E. Mayo, J. S. Takashashi, *Science* **255**, 1581 (1992); M. E. Guido, B. Rusak, H. A. Robertson, *Brain Res.* **739**, 132 (1996).
8. N. Aronin, S. M. Sagar, F. R. Sharp, W. J. Schwartz, *Proc. Natl. Acad. Sci. U.S.A.* **87**, 5959 (1990); D. D. Ginty *et al.*, *Science* **260**, 238 (1993); F. Wollnik *et al.*, *Eur. J. Neurosci.* **7**, 388 (1995).
9. T. Pavlidis, *Biological Oscillators: Their Mathematical Analysis* (Academic Press, New York, 1973).
10. N. Lisitsyn, N. Lisitsyn, M. Wigler, *Science* **259**, 946 (1993).
11. Eighty-four adult male Syrian hamsters (Charles River Laboratories) were entrained to a light-dark cycle (14 hours light, 10 hours dark) for 3 weeks. The hamsters were then transferred to constant dim light (<1 lux) for 7 days, and circadian phases were estimated from spontaneous running-wheel activity (*2*). At CT 19 on the seventh day, half of the hamsters received a light treatment (250 lux, 25 to 35 min), and the other half received a sham treatment (similar handling, but light <1 lux). At the end of the treatment, brains were removed (40 from each group) and placed in phosphate-buffered saline (PBS, 4°C) for 30 s, and a 1.5-mm-thick coronal slice containing the SCN was cut (Stoelting tissue slicer) and transferred to cold PBS. A 1-mm tissue punch (Fine Science Tools USA) containing the SCN was taken, frozen on dry ice, and stored (–70°C). The time between decapitation and freezing of dissected SCNs was 6 to 7 min. Care of hamsters and all procedures were in full compliance with institutional guidelines for animal experimentation.
12. Polyadenylated RNA was prepared from SCN micropunches by guanidinium thiocyanate–CsCl purification followed by oligo-dT chromatography (Oligotex-dT, Qiagen). Oligo-dT–primed, double-stranded cDNA was prepared (Superscript, Gibco-BRL), and the cDNA samples were divided into two and digested with either Rsa I or Alu I, each digest being used for a separate RDA experiment. Fragments were blunt-ligated on each end to a linker containing a Bgl II site [top (A-Bgl-24), 5′-TCCAGCCTCTCACCGCAGATCTGG; bottom, 5′-CCAGATCTGCGGTGAG], and products between 150 and 1500 base pairs were gel-purified; 100 ng of the linked cDNA was used as PCR template in 4 ml of reaction mix, divided into 10 tubes (400 μl each) of PCR buffer (*10*) containing 1.25 μM A-Bgl-24 (top) primer. Samples were warmed to 72°C for 1 min, Amplitaq (Perkin-Elmer, 37.5 U/ml) was added, and 15 cycles (94°C for 1 min, 72°C for 3 min) were performed. Linkers were removed with Bgl II, and fragments from 150 to 1500 base pairs were gel-purified, generating a cDNA representation of the original mRNA to be used as tester or driver in RDA (*10*).
13. RDA was performed essentially as described (*10*), but with the following modifications. Hybridizations were for 40 hours (round 1: driver, 20 μg, tester, 200 ng; round 2: driver, 20 μg, difference product 1, 20 ng; round 3: driver, 20 μg, difference product 2, 500 fg). After round 3, linkers were removed with Bgl II, and PCR products were ligated into PCRscript (Stratagene). For forward subtractions, the cDNA representation from the sham-treated hamsters was used as the driver and that from light-treated hamsters as the tester (*10*); for reverse subtractions, the driver and tester designations were reversed.
14. Duplicate Southern blots of inserts from RDA clones were prepared. Each blot from a duplicate pair was hybridized, respectively, to ^{32}P-labeled cDNA synthesized from +light and –light cDNA representations (*12*) and then washed (twice for 20 min at 65°C, 0.1× SSC, 0.1% SDS). Filters were stripped by boiling and hybridized to subtracted probes; ^{32}P-labeled cDNA was synthesized from final RDA products from the forward and reverse subtractions (*13*), respectively, and washed as above.
15. Forty-one plasmids that were isolated in control reverse subtractions (*13*) or that corresponded to highly abundant transcripts were set aside as likely artifacts; nearly half were accounted for by three clones.
16. Syrian hamsters were entrained to a light-dark cycle (14 hours light, 10 hours dark) for ≥3 weeks, transferred to constant dim light (<1 lux) for 3 to 7 days, subjected to a light or sham treatment (*12*) at CT 19, 14, or 6, anesthetized (sodium pentobarbital, 100 mg/kg intraperitoneally), and intracardially perfused (PBS, then 4% paraformaldehyde-PBS). Brains were removed, postfixed (4% paraformaldehyde-PBS, 10% sucrose, 24 hours), frozen (methylbutane, –20°C, 2 min), and stored (–70°C). Coronal sections (16 μm, cryostat) were cut and prepared as described [D. M. Simmons, J. L. Arriza, L. W. Swanson, *J. Histotechnol.* **12**, 169 (1989)]. Sections were dried and stored (–70°C). In situ hybridization with ^{35}S-labeled riboprobes was as described [D. G. Wilkinson, J. A. Bailes, J. E. Champion, A. P. McMahon, *Development* **99**, 493 (1987)].
17. M. E. Morris, S. Kuhlman, F. C. Davis, C. J. Weitz, unpublished data.
18. The highest scoring matches in BLAST searches [S. F. Altschul, W. Gish, W. Miller, E. W. Myers, D. L. Lipman, *J. Mol. Biol.* **215**, 403 (1990)] for rda-7 ($P = 10^{-22}$) and rda-65 ($P = 10^{-9}$) were to different segments of the 3′ untranslated region of human *egr-3*, starting, respectively, 0.8 kb and 1.5 kb 3′ from the end of the *egr-3* coding sequence.
19. S. Patwardhan *et al.*, *Oncogene* **6**, 917 (1991).
20. J. Honkaniemi, J. Kononen, T. Kainu, I. Pyykonen, M. Pelto-Huikko, *Mol. Brain Res.* **25**, 234 (1994); J. Honkaniemi, S. M. Sagar, I. Pyykonen, K. J. Hicks, F. R. Sharp, *ibid.* **28**, 157 (1995).
21. R. Silver *et al.*, *Neuroreport* **7**, 1224 (1996).
22. J. D. Miller, L. P. Morin, W. J. Schwartz, R. Y. Moore, *Sleep* **19**, 641 (1996).
23. J. A. Treep, H. Abe, B. Rusak, D. M. Goguen, *J. Biol. Rhythms* **10**, 299 (1995).
24. H. Abe, B. Rusak, H. A. Robertson, *Neurosci. Lett.* **127**, 9 (1991); *Brain Res. Bull.* **28**, 831 (1992).
25. Y. Shigeyoshi *et al.*, *Cell* **91**, 1043 (1997).

26. We thank N. Gekakis and D. Staknis for helpful contributions; D. Nathans, M. Greenberg, P. Worley, and A. Lanahan for plasmids; J. Takahashi for a Syrian hamster genomic library; L. Buck for use of her microscope; S. Sullivan for guidance on in situ hybridization; N. Nakanishi and W. Schwartz for helpful suggestions; D. Paul, J. Cohen, and I. Chiu for comments on the manuscript; and L. Ruthig and J. Lee for technical assistance. Supported by a McKnight Scholars Award (C.J.W.), the Council for Tobacco Research–USA, Inc. (C.J.W.), a Stuart H. Q. and Victoria Quan Fellowship in Neurobiology (M.E.M.), and NIH (F.C.D.).

2 October 1997; accepted 8 January 1998

Role of PML in Cell Growth and the Retinoic Acid Pathway

Zhu Gang Wang,* Laurent Delva,* Mirella Gaboli, Roberta Rivi, Marco Giorgio, Carlos Cordon-Cardo, Frank Grosveld, Pier Paolo Pandolfi†

The *PML* gene is fused to the retinoic acid receptor α (*RARα*) gene in chromosomal translocations associated with acute promyelocytic leukemia (APL). Ablation of murine PML protein by homologous recombination revealed that PML regulates hemopoietic differentiation and controls cell growth and tumorigenesis. PML function was essential for the tumor-growth–suppressive activity of retinoic acid (RA) and for its ability to induce terminal myeloid differentiation of precursor cells. PML was needed for the RA-dependent transactivation of the $p21^{WAF1/CIP1}$ gene, which regulates cell cycle progression and cellular differentiation. These results indicate that PML is a critical component of the RA pathway and that disruption of its activity by the PML-RARα fusion protein may be important in APL pathogenesis.

Acute promyelocytic leukemia is a distinct subtype of myeloid leukemia that is invariably associated with chromosomal translocations involving the *RARα* locus (*1*). In 99% of APL cases, *RARα* is fused to the *PML* gene, leading to the production of a PML-RARα chimeric protein (*2*).

Retinoic acid receptors are nuclear hormone receptors that act as RA-inducible transcriptional activators, in their heterodimeric form, with retinoid-X receptors (RXRs), a second class of nuclear retinoid receptors (*3*). Retinoic acid controls fundamental developmental processes, induces terminal differentiation of myeloid hemopoietic progenitors, and has tumor- and cell-growth–suppressive activities (*4*). *PML* is an interferon (IFN)-inducible gene (*5*) that encodes a RING-finger protein typically concentrated within discrete speckled nuclear structures called PML nuclear bodies (PML NBs) or PML oncogenic domains (*2*, *5*). Through its ability to heterodimerize with PML and

Z. G. Wang, L. Delva, M. Gaboli, R. Rivi, M. Giorgio, P. P. Pandolfi, Department of Human Genetics and Molecular Biology Program, Memorial Sloan-Kettering Cancer Center, Sloan-Kettering Division, Graduate School of Medical Sciences, Cornell University, 1275 York Avenue, New York, NY 10021, USA.
C. Cordon-Cardo, Department of Pathology, Memorial Sloan-Kettering Cancer Center, 1275 York Avenue, New York, NY 10021, USA.
F. Grosveld, Department of Cell Biology and Genetics, Faculty of Medicine, Erasmus University, Post Office Box 1738, 3000 DR, Rotterdam, Netherlands.

*These authors contributed equally to this work.
†To whom correspondence should be addressed. E-mail: p-pandolfi@ski.mskcc.org

RXR, PML-RARα is thought to interfere with both PML and RAR/RXR-RA pathways, thus acting as a double dominant negative oncogenic product (5, 6). However, the normal function of PML and its contribution to APL pathogenesis are unknown.

To investigate these aspects, we disrupted the *PML* gene in the mouse germ line (7, 8). By homologous recombination in murine embryonic stem (ES) cells, we substituted part of exon 2 of the *PML* gene, which encodes the RING-finger domain, with a neomycin resistance gene cassette (Fig. 1, A to C). Mice homozygous for the PML mutation ($PML^{-/-}$) were born with the expected Mendelian frequency, were indistinguishable at the gross phenotypic level from $PML^{+/+}$ and $PML^{+/-}$ littermates, and were fertile; however, the $PML^{-/-}$ mice were extremely susceptible to spontaneous Botryomycotic infections (9). Successful disruption of the *PML* gene was inferred from the lack of *PML* mRNA and PML NBs in mouse primary embryonic fibroblasts (MEFs) from $PML^{-/-}$ embryos (Fig. 1, D and E) (7).

Analysis of peripheral blood (PB) from $PML^{-/-}$ mice (10) revealed a marked reduction of circulating granulocytes (neutrophils: $PML^{+/+}$, 1518 ± 220 cells/μl; $PML^{-/-}$, 795 ± 243 cells/μl; $P < 0.02$; basophils: $PML^{+/+}$, 247 ± 169 cells/μl; $PML^{-/-}$, 69 ± 19 cells/μl; $P < 0.01$; eosinophils: $PML^{+/+}$, 478 ± 142 cells/μl; $PML^{-/-}$, 136 ± 74 cells/μl; $P < 0.03$) and an overall reduction of circulating myeloid cells (monocytes: $PML^{+/+}$, 365 ± 196 cells/μl; $PML^{-/-}$, 203 ± 77 cells/μl; $P < 0.05$), which caused leukopenia. Flow-cytometric analysis of cells from the spleen, lymph nodes, thymus, and bone marrow (BM) and differential counts of BM cells demonstrated a reduction of both granulocytes and monocytes in the BM of $PML^{-/-}$ mice (11). Thus, $PML^{-/-}$ mice have an impaired capacity for terminal maturation of their myeloid cells.

PML overexpression in cultured cells is accompanied by growth inhibition (12). To assess the effects of PML inactivation on cell proliferation, we studied the growth of early passages of MEFs (13), which normally express PML (Fig. 1E) and whose proliferative properties are well characterized (14). At low density, $PML^{+/+}$, $PML^{+/-}$, and $PML^{-/-}$ cultures were morphologically indistinguishable. However, $PML^{-/-}$ MEFs grew faster than $PML^{+/+}$ MEFs (Fig. 2A), as confirmed by ^{3}H-labeled thymidine incorporation (Fig. 2B). $PML^{+/-}$ MEFs showed an intermediate growth rate (Fig. 2, A and B). In situ terminal deoxynucleotidyl tranferase labeling experiments revealed comparable numbers of apoptotic cells (15). Furthermore, PML inactivation markedly enhanced the ability of MEFs to form colonies (Fig. 2C). The S phase population of $PML^{-/-}$ MEFs was increased with a concomitant decrease in the G_0/G_1 population (Fig. 2D), a change analogous to that observed in retinoblastoma$^{-/-}$ MEFs (14). $PML^{-/-}$ MEF monolayers achieved higher cellular densities and formed foci (Fig. 2, E

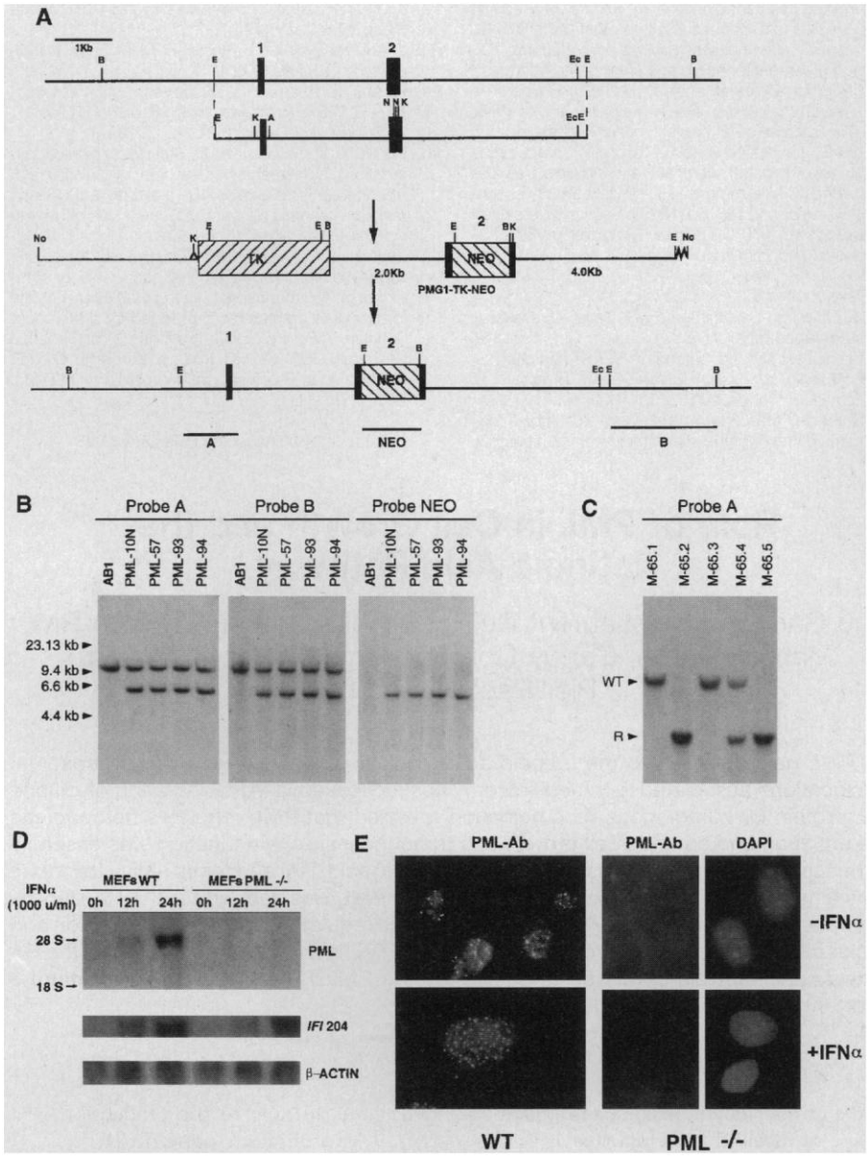

Fig. 1. Targeted disruption of the *PML* gene. (**A**) Map of the murine 5′ *PML* genomic region determined by restriction mapping, Southern blot hybridization, and DNA sequencing (15). The targeting vector is derived from a 6.8-kb Eco RI fragment of the *PML* gene. The TK and Neo selectable markers are shown as hatched boxes (7). Also shown is the endogenous *PML* genomic region after correct integration of the targeting construct by homologous recombination and the three probes used for Southern blot analysis (solid lines) (7). E, Eco RI; K, Kpn I; N, Nar I; No, Not I; A, Apa I; B, Bam HI; and Ec, Eco RV. (**B**) Southern blot analysis with A, B, and Neo probes of Bam HI–digested DNA from recombined ES cell clones and AB1 untransfected ES cells confirms proper recombination. (**C**) Southern blot analysis with the probe A of Eco RI–digested tail DNA from littermates obtained from intercrossing two $PML^{+/-}$ mice. DNAs from two mice show the disappearance of the wild-type (WT) band. *R*, recombinant bands. (**D**) Northern blot showing that the homozygous *PML* mutation abolishes *PML* mRNA expression. For up-regulation of *PML* expression, $PML^{-/-}$ and $PML^{+/+}$ MEFs were treated with murine IFNα+β. The integrity and amount of RNA as well as stimulation by IFNs were shown by rehybridizing the same blot with β-actin and IFI 204 probes; h, hours; 28 S and 18 S, ribosomal RNA. (**E**) $PML^{-/-}$ and $PML^{+/+}$ MEFs were studied by immunofluorescence in basal conditions or upon IFN treatment for 24 hours (7). $PML^{-/-}$ MEFs do not show any PML nuclear staining. The nuclei of the $PML^{-/-}$ cells were visualized by costaining with 4′6′-diamidino-2-phenylindole (DAPI) (right). PML-Ab, PML rabbit antiserum.

and F) but, unlike fully transformed cells, were unable to grow in a semisolid medium.

These findings suggest that PML is a negative growth regulator and therefore may function as a tumor suppressor. Although the incidence of spontaneous tumors in the $PML^{-/-}$ cohort was not increased during the first year of life, mutant mice succumbed to infections, severely compromising the long-term assessment of tumor incidence (9). We therefore studied tumorigenesis in two experimental models designed to accelerate tumor formation (16, 17). In the first, we exposed the skin of mice [because PML is highly expressed in keratinocytes (Fig. 3B)] to a single application of the tumor initiator dimethybenzanthracene (DMBA) followed by treatment for several weeks with the tumor promoter 12-0-tetradecanoylphorbol-13-acetate (TPA), a protocol that gives rise to papillomas that occasionally progress to carcinomas after several months (16). $PML^{-/-}$ mice developed more papillomas (Fig. 3A), although the frequency of tumors undergoing malignant transformation was similar in the two groups ($PML^{+/+}$, 1.8%; $PML^{-/-}$, 2.3%). In the second model, DMBA was injected into the salivary gland of $PML^{-/-}$ and $PML^{+/+}$ mice, a procedure that normally produces sarcomas and fibrosarcomas (16, 17). $PML^{-/-}$ mice developed more tumors than control mice (greater than twofold; $P < 0.04$) (Fig. 3, D to I) (16). Unexpectedly, 50% of the tumors observed in the $PML^{-/-}$ group were T and B cell lymphomas (only one B cell lymphoma arose in the wild-type cohort; $P < 0.02$), and 21% were fibrohistiocytoma-like lesions (rare tumors with a histiocytic-macrophagic cellular component) (Fig. 3E). Lymphomas in $PML^{-/-}$ mice were aggressive metastatic malignancies (Fig. 3D). They appeared to be of clonal origin because the infiltrating lymphoid population homogeneously expressed either CD4 or CD8 markers (T lymphomas) and either κ or λ chains (B lymphomas) (Fig. 3, H and I). Macrophage tumoricidal activity, natural killer cell, and cytotoxic T lymphocyte activities, which are required for efficient surveillance against tumors, were normal in $PML^{-/-}$ mutants (9); however, upon concanavalin A activation, splenic lymphocytes in $PML^{-/-}$ mutants showed a proliferative advantage despite normal production of interleukin-10 (IL-10), IL-4, IL-6, and IFN-γ (15). PML can, therefore, antagonize the initiation, promotion, and progression of tumors of different histological origins.

We next investigated whether PML was required for the growth-suppressive activity of RA. Retinoic acid markedly inhibited the growth of $PML^{+/+}$ MEFs but had little effect on the growth of $PML^{-/-}$ MEFs (Fig. 4, A and B). Treatment with RA did not increase cell death in these experiments (15).

Because RA induces terminal myeloid and granulocytic differentiation (3, 4, 18), we tested whether the reduction in myeloid cells in the $PML^{-/-}$ mice resulted from an impaired response of $PML^{-/-}$ progenitors to RA (19). In in vitro methylcellulose colony assays of hemopoietic progenitors, BM cells from $PML^{-/-}$ and $PML^{+/+}$ mice were comparable in their ability to form erythroid and myeloid colonies (Fig. 4C). In the presence of RA, the number of myeloid colonies obtained from the $PML^{+/+}$ progenitors was increased as expected (18, 19), but this effect was completely abrogated in $PML^{-/-}$ cells (Fig. 4D). Thus, the presence of PML is crucial for the growth-inhibitory activity of RA, as well as for RA induction of myeloid differentiation.

To determine if PML-RARα could restore RA activity, we evaluated the RA responsiveness of BM cells from $PML^{-/-}$ PML-RARα transgenic mice (19). We obtained these mutants by crossing $PML^{-/-}$ mice with PML-RARα transgenic mice that express the fusion gene only in the myeloid promyelocytic compartment (19). Retinoic acid significantly reduced the number of myeloid colonies derived from $PML^{-/-}$ PML-RARα BM cells, suggesting that PML-RARα can directly mediate RA growth-inhibitory activity in a PML-independent manner (Fig. 4D).

To explore the mechanism by which PML mediates RA function, we tested whether

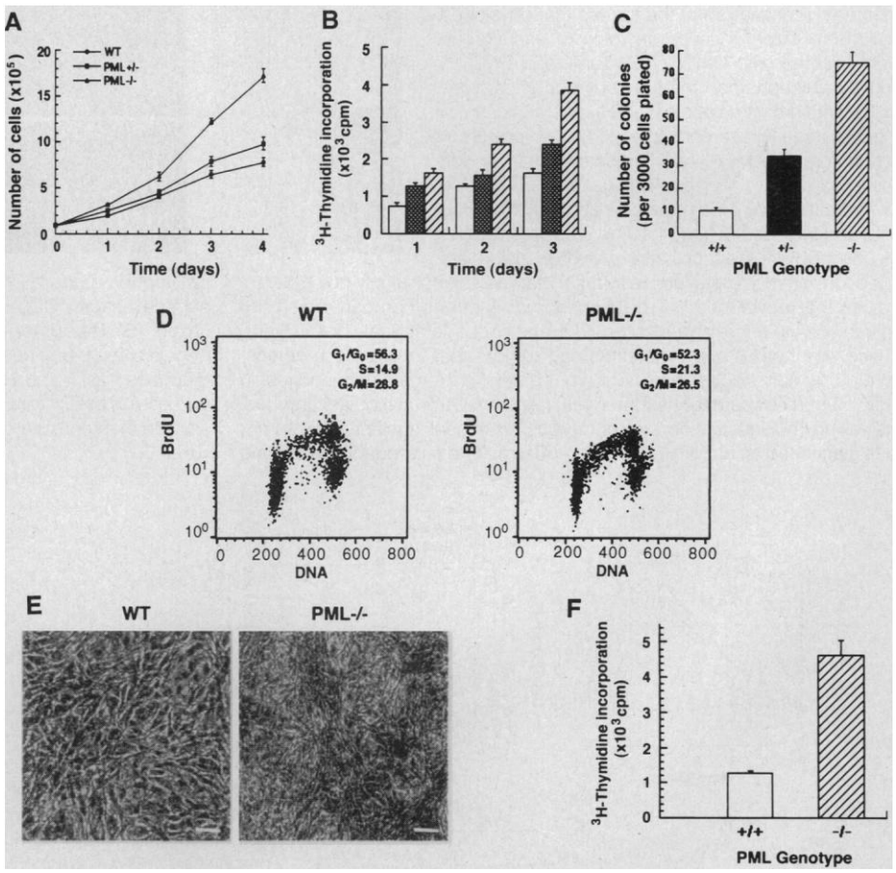

Fig. 2. Growth properties of MEFs of different PML genotypes. (**A**) Growth curves. Each time point is the average of triplicate measurements. Doubling time of MEFs: $PML^{-/-}$, 26.4 ± 3.1 hours; $PML^{+/-}$, 29.8 ± 3.3 hours; $PML^{+/+}$, 32.9 ± 3.9 hours (13). (**B**) [^{3}H]thymidine incorporation. Cells (5 x 10^3 per well) were distributed in 96-well plates and cultured in the presence of [^{3}H]thymidine. Each time point is the average of triplicate measurements (13). $PML^{+/+}$, open bars; $PML^{+/-}$, solid bars; $PML^{-/-}$, hatched bars. (**C**) Clonogenic efficiency (13). The colonies (>10 cells) were scored under the microscope 8 days after plating. The scoring of colonies at day 16, when the colonies were bigger in size and detectable by the eye, gave superimposable results. (**D**) Analysis of cell cycle stages in $PML^{+/+}$ (left) and $PML^{-/-}$ (right) MEFs. Cultures were pulsed with BrdU, labeled with an antibody to BrdU to detect DNA synthesis (vertical axis) and propidium iodide to detect total DNA (horizontal axis), and analyzed by two-dimensional flow cytometry (13). (**E**) Loss of contact inhibition in $PML^{-/-}$ MEFs. Cells were seeded at 3 × 10^5 cells in 60-mm dishes and, after 2 weeks, fixed and stained. $PML^{-/-}$ MEFs grew to a higher density than $PML^{+/+}$ MEFs of the same passage. Scale bar, 60 μm. (**F**) [^{3}H]thymidine incorporation of $PML^{-/-}$ and $PML^{+/+}$ MEFs cultured at confluence. The conditions were as in (B), except that 4 × 10^4 cells per well were seeded.

PML is required for the RA-dependent transactivation of the cyclin-dependent kinase inhibitor $p21^{WAF1/CIP1}$ gene, which can be activated by nuclear receptors, including RXRα/RARα (*20*). We transfected $PML^{-/-}$ and $PML^{+/+}$ MEFs with a $p21^{WAF1/CIP1}$ promoter-reporter construct and assessed the response to RA treatment. Consistent with previous results (*20*), RA stimulated in

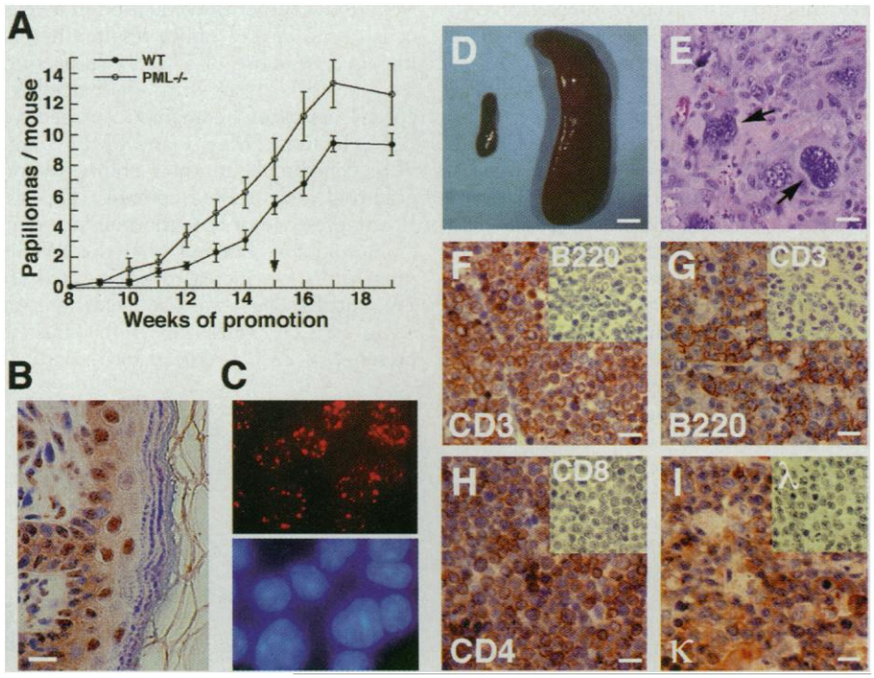

Fig. 3. Role of PML in tumorigenesis. (**A**) Rate of appearance of papillomas in $PML^{-/-}$ (n = 14) and $PML^{+/+}$ (n = 14) mice treated with DMBA and TPA. Graph shows the average number of papillomas ± SE, and the arrow indicates the time when the tumor promotion treatment with TPA was terminated. One of two independent experiments is shown (*16*). (**B** and **C**) PML expression in the skin and lymphocytes. (B) Immunohistochemical analysis of the skin was performed on paraffin tissue sections from newborn mice with a PML rabbit antiserum (*7*). PML is readily detectable in its nuclear speckled configuration in keratinocytes. Scale bar, 50 μm. (C) Splenic lymphocytes were studied by immunofluorescence (*7*) (top). Nuclei were visualized by DAPI (bottom). PML NBs are detectable in all lymphocytes. PML is also expressed in thymic and BM lymphocytes (*15*). (**D** and **E**) Histopathological analysis of the tumors that developed in $PML^{-/-}$ mice. Twenty-five mice of each group were injected with DMBA (*16*). Tumors in $PML^{-/-}$ [four T cell lymphomas, three B cell lymphomas, three malignant fibrohistocytomas (MFH), one angiosarcoma, and three fibrosarcomas] and $PML^{+/+}$ [one B cell lymphoma, one MFH, two fibrosarcomas, two soft tissue sarcomas, and one benign papilloma] mice were identified by external examination after 4.86 ± 0.53 and 5.67 ± 0.69 months ($P < 0.02$), respectively, upon DMBA injection, after which animals were killed for pathological examination. (D) Marked splenomegaly in a $PML^{-/-}$ mouse that developed a T cell lymphoma (right), as compared with the spleen of a wild-type age-matched control mouse (left). Scale bar, 0.5 cm. These lymphomas were metastasizing tumors that involved the spleen, thymus, lymph nodes, liver, and vertebrae. (E) Hematoxylin and eosin staining of a subcutaneous tumor with large dysplatic histiocytes (arrows) displaying multinucleation and numerous prominent nucleoli. This tumor was diagnosed as an MFH. Scale bar, 50 μm. (**F** to **I**) Immunophenotyping of lymphomas from $PML^{-/-}$ mice. (F) The tumor is positive for the T cell surface antigen CD3 and negative for the B cell surface antigen B220 (inset). (G) The tumor is positive for the B cell surface marker B220 and negative for the T cell surface antigen CD3 (inset). These tumors were diagnosed as T and B cell lymphomas, respectively. The homogeneous expression of CD4 or CD8 (T lymphomas) (H) and κ or λ (B lymphomas) (I) surface markers supports the clonal origin of these tumors. Scale bars, 25 μm.

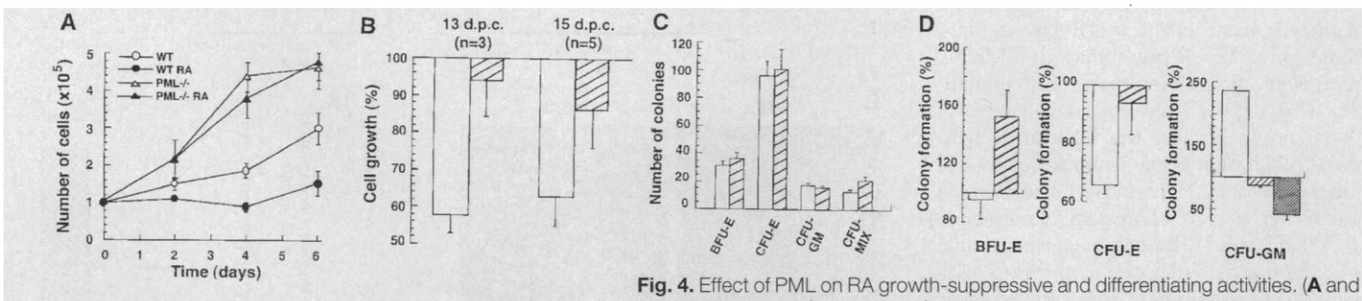

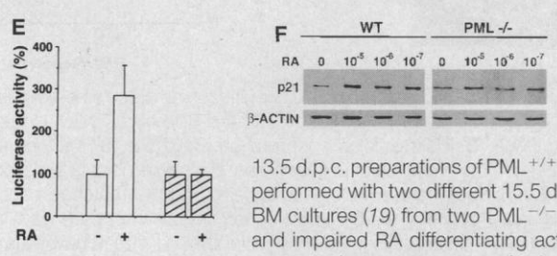

Fig. 4. Effect of PML on RA growth-suppressive and differentiating activities. (**A** and **B**) Growth of $PML^{+/+}$ and $PML^{-/-}$ MEFs in the presence of RA. (A) Each time point is the average of triplicates from a 13.5 days post coitum (d.p.c.) early passage preparation of $PML^{+/+}$ and $PML^{-/-}$ MEFs. Cells were cultured with or without 1 μM RA. (B) The data are expressed as a percentage of growth of RA-treated versus untreated cells (untreated = 100% of growth), at day 6 of culture. The values are averages calculated from triplicates of three (n = 3) experiments performed with 13.5 d.p.c. preparations of $PML^{+/+}$ (open bars) and $PML^{-/-}$ (hatched bars) MEFs and five (n = 5) independent experiments performed with two different 15.5 d.p.c. preparations of $PML^{+/+}$ and $PML^{-/-}$ MEFs. (**C**) Hemopoietic colonies from in vitro BM cultures (*19*) from two $PML^{-/-}$ and two $PML^{+/+}$ mice, scored in triplicate, are shown. Bars are as in (B). (**D**) Aberrant and impaired RA differentiating activity in $PML^{-/-}$ and $PML^{-/-}$ PML/RARα hemopoietic progenitors (*19*). The data are expressed as a percentage of colony formation of RA-treated (1 μM) versus untreated cells (untreated = 100%). The bars indicate the mean values ± SD. Triplicate measurements from two $PML^{-/-}$ (hatched bars), two $PML^{+/+}$ (open bars), and two $PML^{-/-}$ PML/RARα (solid bar) mice are shown. (**E**) $PML^{-/-}$ and $PML^{+/+}$ MEFs were transiently transfected by calcium phosphate precipitation with the $p21^{WAF1/CIP1}$ promoter-luciferase reporter plasmid pGL2 (10 μg per transfection) (*20*), together with TK–β-galactosidase (2 μg), in the presence or absence of 1 μM RA. Transactivation is expressed as a percentage of luciferase activity, as deduced from arbitrary light units normalized to β-galactosidase activity. The values shown are averages ± SD calculated from triplicate platings, from one representative experiment out of three. Bars are as in (B). (**F**) Protein immunoblot analysis of $p21^{WAF1/CIP1}$ expression in $PML^{-/-}$ and $PML^{+/+}$ BM cells upon treatment with RA at concentrations of 10^{-5} M, 10^{-6} M, or 10^{-7} M for 72 hours.

$PML^{+/+}$ MEFs the basal activity of the $p21^{WAF1/CIP1}$ promoter by two to three times (Fig. 4E). In the absence of PML, the RA-dependent transactivation of the promoter was fully abrogated (Fig. 4E). Accordingly, concentrations of RA at 10^{-7} or 10^{-6} M did not activate the endogenous $p21^{WAF1/CIP1}$ gene in $PML^{-/-}$ BM cells (Fig. 4F). Thus, PML is essential for the RA-dependent induction of $p21^{WAF1/CIP1}$. Because $p21^{WAF1/CIP1}$ up-regulation can result in terminal differentiation of hemopoietic cells (*20*), the lack of $p21^{WAF1/CIP1}$ induction in $PML^{-/-}$ cells might partially explain the role of PML in controlling hemopoietic cell differentiation.

Our findings demonstrate that PML controls cell proliferation, tumorigenesis, and the differentiation of hemopoietic precursors. These functions are, at least in part, based on the ability of PML to interact with the RA pathway and in particular its ability to mediate RA growth-suppressive and differentiating activities. Preliminary results indicate that PML can be part of the RXR/RAR transcription complex (*21*), providing a direct explanation for its effect on RA function. This function is consistent with the role of PML in the RA-dependent transactivation of specific genes such as $p21^{WAF1/CIP1}$ and with the development of T and B cell lymphomas in mice deficient in RARα (*22*). These results provide a framework for understanding the molecular pathogenesis of APL. Whereas APL might result from the functional interference of PML-RARα with two independent pathways, PML and RXR/RAR, we show here that these proteins act, at least in part, in the same pathway. Thus, by simultaneously interacting with RXR and PML, PML-RARα may inactivate this pathway at multiple levels, leading to the proliferative advantage and the block of hemopoietic differentiation that characterize APL.

REFERENCES AND NOTES

1. F. Grignani *et al.*, *Blood* **83**, 10 (1994); P. P. Pandolfi, *Haematologica* **81**, 472 (1996).
2. L. Longo *et al.*, *J. Exp. Med.* **172**, 1571 (1990); J. Borrow, A. D. Goddard, D. Sheer, E. Solomon, *Science* **249**, 1577 (1990); H. de Thé, C. Chomienne, M. Lanotte, L. Degos, A. Dejean, *Nature* **347**, 558 (1990); P. P. Pandolfi *et al.*, *Oncogene* **6**, 1285 (1991); H. de Thé *et al.*, *Cell* **66**, 675 (1991); A. Kakizuka *et al.*, *ibid.*, p. 663; A. D. Goddard, J. Borrow, P. S. Freemont, E. Solomon, *Science* **254**, 1371 (1991); P. P. Pandolfi *et al.*, *EMBO J.* **11**, 1397 (1992).
3. P. Chambon, *FASEB J.* **10**, 940 (1996).
4. M. A. Smith, D. R. Parkinson, B. D. Cheson, M. A. Friedman, *J. Clin. Oncol.* **10**, 839 (1992); L. J. Gudas, M. B. Sporn, A. B. Roberts, *The Retinoids: Cellular Biology and Biochemistry of the Retinoids* (Raven, New York, 1994).
5. J. Dyck *et al.*, *Cell* **76**, 333 (1994); K. Weis *et al.*, *ibid.*, p. 345; M. H. M. Koken *et al.*, *EMBO J.* **13**, 1073 (1994); M. Stadler *et al.*, *Oncogene* **11**, 2565 (1995); C. Lavau *et al.*, *ibid.*, p. 871; K. Nason-Burchenal *et al.*, *Blood* **88**, 3926 (1996).
6. P. Kastner *et al.*, *EMBO J.* **11**, 629 (1992); A. Perez *et al.*, *ibid.* **12**, 3171 (1993); F. Grignani *et al.*, *Cell* **74**, 423 (1993).
7. PML phage clones were obtained from a 129Sv mouse strain genomic library. The targeting vector contains herpes simplex virus–thymidine kinase (TK) and TK-Neo selectable markers (*8*), the latter of which replaces 94 base pairs of *PML* exon 2 encoding the PML RING-finger domain [M. Fagioli *et al.*, *Oncogene* **7**, 1083 (1992)], and is flanked by a 2.0-kb Apa I–Nar I fragment containing *PML* intron 1 and a small portion of exon 2 and a 4.0-kb Nar I–Eco RI fragment corresponding to a part of *PML* exon 2 and intron 2. The Not I linearized vector was electroporated into AB1 ES cells, and double selection was carried out as described (*8*). Resistant clones were screened by Southern (DNA) blotting with the 5′ and 3′ external and internal probes, as shown in Fig. 1A. Germline-transmitting chimeric males obtained from two independent $PML^{+/-}$ euploid ES cell clones were bred with 129Sv females to generate $PML^{+/-}$ mice for intercrossing. A PML rabbit antiserum was used for detection of the endogenous murine PML protein [K. L. B. Borden *et al.*, *EMBO J.* **14**, 1532 (1995)].
8. P. P. Pandolfi *et al.*, *Nature Gen.* **11**, 40 (1995).
9. M. Gaboli *et al.*, in preparation.
10. Peripheral blood counts were performed for $PML^{+/+}$ (n = 28) and $PML^{-/-}$ (n = 20) sex- and age- (2 to 3 months old) matched syngeneic (129Sv) littermates. Differential counts of myeloid and lymphoid subpopulations from $PML^{+/+}$ (n = 24) and $PML^{-/-}$ (n = 22) mice were carried out on Wright-Giemsa–stained PB smears. Differential counts of three or four smears per animal were scored for a total of at least 300 cells.
11. The following antibodies (PharMingen, San Diego, CA) in single or double staining were used for flow-cytometric analysis: hemopoietic stem cells or progenitors (c-Kit and CD34), T lymphocytes [Thy1, CD4, CD8, CD3, CD2, CD24, T cell receptor (TCR) αβ, and TCRγδ], B lymphocytes (CD2, CD24, B220, and αIγ), and myeloid cells (Mac-1, Gr-1, and Ly-6C). If required, cells were preincubated with an antibody to mouse FcγII/III receptors (Fc Block); 10^5 cells from $PML^{+/+}$ (n = 9) and $PML^{-/-}$ (n = 9) sex- and age-matched syngeneic (129Sv) littermates were analyzed in three independent experiments. The reduction of granulocytes and monocytes in the BM of $PML^{-/-}$ mice was demonstrated by a 10 to 20% reduction of Mac-1–positive ($P < 0.03$) or Gr-1–positive ($P < 0.02$) (monocytic and granulocytic), Mac-I–positive and Gr-1–positive ($P < 0.01$) (granulocytic), and Mac-1–positive and Gr-1–negative ($P < 0.02$) or Ly-6C–positive ($P < 0.03$) (monocytic) cells. No other difference was observed with any other antibody. Differential counts on cytospin smears also showed a marked reduction of granulocytes ($PML^{-/-}$, 12 ± 3%; $PML^{+/+}$, 29 ± 5%; $P < 0.01$) and monocytes ($PML^{-/-}$, 0.1 ± 0.1%; $PML^{+/+}$, 0.5 ± 0.2%; $P < 0.02$) in the BM of $PML^{-/-}$ mice, with no notable decrease or accumulation of early hemopoietic precursors (blasts + promyelocytes + metamyelocytes + myelocytes) ($PML^{-/-}$, 5.2 ± 2%; $PML^{+/+}$, 5.6 ± 1.7%) and a relative increase of erythroblasts.
12. Z. M. Mu, K. V. Chin, J. H. Liu, G. Lozano, K. S. Chang, *Mol. Cell. Biol.* **14**, 6858 (1994); M. H. M. Koken *et al.*, *Oncogene* **10**, 1315 (1995); J. H. Liu, Z. M. Mu, K. S. Chang, *J. Exp. Med.* **181**, 1965 (1995); X. F. Le, P. Yang, K. S. Chang, *J. Biol. Chem.* **271**, 130 (1996).
13. Mouse primary embryonic fibroblasts were isolated from embryos at 13.5 or 15.5 days of gestation. For growth curve experiments, 10^5 cells per well were seeded in six-well plates in Dulbecco's minimum essential medium with 20% fetal bovine serum (FBS) and counted. Nine independent experiments were carried out from three different MEF preparations. Doubling time was calculated from the slope of the best fit line of the logarithm of cell number as a function of time. DNA synthesis was measured by incorporation of [^{3}H]thymidine (2 μCi/ml) in five independent experiments. For clonogenic efficiency, 3×10^3 MEFs, in three independent experiments, were distributed on 60-mm dishes, and the number of colonies (>10 cells) was scored after 8 and 16 days (*14*). For cell cycle analysis, subconfluent cultures of MEFs were labeled for 4 hours with 10 μM bromodeoxyuridine (BrdU) (Sigma) and analyzed by two-dimensional flow cytometry (*14*).
14. S. D. Conzen and C. N. Cole, *Oncogene* **11**, 2295 (1995); M. Serrano *et al.*, *Cell* **85**, 27 (1996).
15. Z. G. Wang and P. P. Pandolfi, unpublished data.
16. The backs of $PML^{+/+}$ and $PML^{-/-}$ sex- and age- (6 to 10 weeks old) matched syngeneic (129Sv) littermates (n = 24 for each group in two different experiments) were treated with a single application of DMBA (25 μg in 200 μl of acetone) followed by biweekly application of TPA (200 μl of 0.1 μM solution in acetone) [C. J. Kemp, L. A. Donehower, A. Bradley, A. Balmain, *Cell* **74**, 813 (1993)]. Treatment with TPA was terminated after 15 weeks. The number of papillomas (over 2 mm in diameter) on each mouse was scored weekly. All papillomas were taken for histological examination 36 weeks after the initiation with DMBA. The difference in the number of papillomas observed in $PML^{-/-}$ and $PML^{+/+}$ mice was statistically significant from the 12th week of promotion (P values: 12th week, $P < 0.01$; 13th week, $P < 0.02$; 14th week, $P < 0.01$; 15th week, $P < 0.05$; 16th week, $P < 0.01$; 17th week, $P < 0.02$). The effects of a systemic dose of DMBA were studied as follows: DMBA (2.5 mg in 50 μl of liquid petrolatum) was injected into the left lobe of the surgically exposed salivary gland of $PML^{-/-}$ (n = 25) and $PML^{+/+}$ (n = 25) sex- and age- (6 to 10 weeks old) matched syngeneic (129Sv) anesthetized littermates in two different experiments. Mice were followed for 1 year and then killed. Postmortem analysis revealed that tumors in $PML^{-/-}$ mutants developed in mice that had not yet developed infections.
17. T. Barka, H. van der Noen, A. M. Michelakis, I. Schenkein, *Lab. Invest.* **42**, 656 (1980).
18. D. Douer and H. P. Koeffler, *Exp. Cell. Res.* **138**, 193 (1982); C. Gratas, M. L. Menot, C. Dresch, C. Chomienne, *Leukemia* **7**, 1156 (1993).
19. To score for colony-forming units–erythrocyte (CFU-E), we plated BM cells at a concentration of 2×10^5 cells per dish in MethoCult M3330 (Stemcell Technology, Vancouver, Canada) and counted colonies after 2 days. For burst-forming units–erythrocyte (BFU-E), CFU–granulocyte and monocyte (CFU-GM), and CFU–granulocyte, monocyte, erythrocyte, and megakaryocyte (CFU-MIX), BM cells were plated at a concentration of 3×10^4 cells per dish in MethoCult M3430 (Stemcell Technology). Colonies were scored at days 7 and 14. Five independent experiments were carried out from $PML^{-/-}$ (n = 7) and $PML^{+/+}$ (n = 7) sex- and age-matched syngeneic littermates. BM cultures with or without RA: To score CFU-E and BFU-E, we plated BM cells as above and counted them at days 2 and 6, respectively; for CFU-GM, 5×10^4 cells were plated in medium with 30% FBS, granulocyte and monocyte colony-stimulating factor (GM-CSF) (20 ng/ml), and granulocyte CSF (G-CSF) (50 ng/ml) and scored after 6 days. Retinoic acid in dimethyl sulfoxide (DMSO) was added at a final concentration of 1 μM. Untreated cells were cultured in the presence of the same concentration of DMSO. $PML^{-/-}$ PML-RARα BM cells were harvested from mice obtained by intercrossing $PML^{-/-}$ mice and PML-RARα transgenic mice [L. Z. He *et al.*, *Proc. Natl. Acad. Sci. U.S.A.* **94**, 5302 (1997)]. These experiments were performed on healthy mice before the occurrence of leukemia. Nine independent experiments were carried out from $PML^{-/-}$ (n = 11), $PML^{+/+}$ (n = 11), and $PML^{-/-}$ PML-RARα (n = 2) sex- and age-matched syngeneic littermates.
20. M. Liu, M. H. Lee, M. Cohen, M. Bommakanti, L. P. Freedman, *Genes Dev.* **10**, 142 (1996); M. Liu, A. Iavarone, L. P. Freedman, *J. Biol. Chem.* **271**, 31723 (1996).
21. L. Delva *et al.*, in preparation.
22. T. Manshouri *et al.*, *Blood* **89**, 2507 (1997).

23. We thank M. Barna, A. Bradley, A. Bygrave, G. Cattoretti, R. Dalla Favera, T. Delohery, E. Dzierzak, M. Fagioli, P. S. Freemont, D. Gandini, N. Hawe, M. Lindenbaum, L. Longo, R. Lovell-Badge, L. Luzzatto, S. Nicolis, P. G. Pelicci, and E. Solomon for materials, assistance, and advice. Partially supported by the Associazione Italiana per la Ricerca sul Cancro (P.P.P., R.R., and M.G.) and the Ligue Nationale contre le Cancer of France (L.D.). P.P.P. is a Scholar of the Leukemia Society of America. Supported by the Sloan-Kettering Institute (CA-08748) and National Institutes of Health (CA 71692 awarded to P.P.P.).

5 September 1997; accepted 16 January 1998